



The construction of aggregation-induced charge transfer emission systems in aqueous solution directed by supramolecular strategy

Weirui Qian^a, Minzan Zuo^b, Pengbo Niu^a, Xiao-Yu Hu^{b,*}, Leyong Wang^{a,c,*}

^a Key Laboratory of Mesoscopic Chemistry of MOE, Jiangsu Key Laboratory of Advanced Organic Materials, School of Chemistry and Chemical Engineering, Nanjing University, Nanjing 210023, China

^b College of Materials Science and Technology, Nanjing University of Aeronautics and Astronautics, Nanjing 211106, China

^c Department of Chemistry, Xihua University, Chengdu 610039, China

ARTICLE INFO

Article history:

Received 3 August 2021

Revised 18 September 2021

Accepted 22 September 2021

Available online 26 September 2021

Keywords:

Aggregation-induced charge transfer emission

Supramolecular strategy

Long luminescence lifetime

Self-assembly

Co-aggregate

ABSTRACT

Novel aggregation-induced charge transfer (CT) emission systems with long luminescence lifetime directed by supramolecular strategy have been successfully developed in water. The dimethylacridine-based electron donor (**BrAc**) with excellent aggregation ability can co-aggregate with a triazine-based electron acceptor (**TRZ**) to form nanorods in water, which exhibit CT emission with long lifetime ($\tau = 0.92 \mu\text{s}$). As for a similar electron donor (**QaAc**) with poor aggregation ability, water-soluble pillar[5]arene (**WP5**) can be introduced to promote the aggregation process, leading to the obvious CT emission with long lifetime ($\tau = 0.61 \mu\text{s}$). In addition, structural modification of the acceptor with substituent groups possessing stronger electron-accepting capabilities will cause red-shift (about 50 nm) of the emission, which allows conveniently constructing long lifetime organic luminescent materials with different emission colors.

© 2021 Published by Elsevier B.V. on behalf of Chinese Chemical Society and Institute of Materia Medica, Chinese Academy of Medical Sciences.

Organic luminescent materials directed by supramolecular strategy in aqueous solution have been widely investigated in recent years [1–6]. Based on this design, different types of molecules can be noncovalently incorporated into the formed nanoaggregates through weak intermolecular interactions, which can avoid multiple steps of synthesis and purification during the structure fabrication. In addition, these highly ordered nanoaggregates can effectively shorten the distance between the donor and acceptor to ensure efficient energy transfer (ET) or charge transfer (CT), which provide a convenient way for fabricating functional nanosystems [7–11]. For example, in our previous work, a highly efficient energy transfer (ET) system based on the self-assembly of a water-soluble pillar[5]arene (**WP5**), a bis(4-phenyl)acrylonitrile derivative (BPT), and two types of fluorescence dye was successfully fabricated, and it showed potential application in artificial light-harvesting [7]. However, these ET systems are usually emissive with very short luminescence lifetime ($\tau < 10 \text{ ns}$), as the same level as the autofluorescence from organisms, which greatly limits their applications in the field such as time-resolved luminescence imaging [12–16].

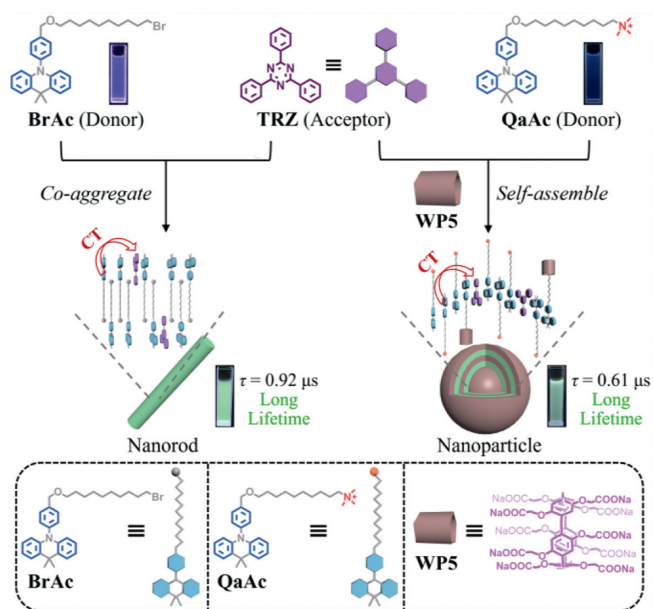
Comparing with ET materials, charge transfer (CT) materials with long luminescence lifetime at the microsecond level have al-

ways been a research hotspot for scientists, owing to their wide applications in many fields such as organic light-emitting diodes, time-resolved luminescence imaging, and photocatalytic synthesis [17–20]. In the construction of CT molecules, electron donor (D) and acceptor (A) are often linked through conjugated bonds to ensure efficient charge transfer [21–24]. However, the resulted through-bond charge transfer (TBCT) effect tends to induce a large red-shift of the emission, which is undesired for the construction of short-wavelength CT materials [25]. Recently, a new construction strategy for CT materials with long lifetime has aroused great interests, in which D and A units are non-conjugated but spatially proximate. For example, Wang *et al.* developed a kind of CT polymers based on non-conjugated polyethylene backbones with through-space charge transfer (TSCT) effect between pendant D and A units [26]. Such TSCT effect cannot only ensure efficient charge transfer, but also can avoid the large red-shift of emission for the conjugated architectures [27–29]. However, among those reported CT materials with TSCT effect, D and A units are still covalently connected based on complicated synthesis procedures to ensure efficient charge transfer, which greatly limits the design of various novel CT materials. From this perspective, delicate design of CT materials with long lifetime directed by supramolecular strategy featuring non-covalent interactions and structural diversity is highly appealing.

Herein, different aggregation-induced charge transfer (CT) emission systems with long lifetime directed by supramolecular

* Corresponding authors.

E-mail addresses: huxy@nuaa.edu.cn (X.-Y. Hu), lywang@nju.edu.cn (L. Wang).



Scheme 1. Schematic illustration of the aggregation-induced charge transfer emission systems in water directed by supramolecular strategy.

strategy have been successfully developed in aqueous phase (Scheme 1). A dimethylacridine-based derivative (**BrAc**) with excellent aggregation ability was designed as the electron donor, which could co-aggregate with the triazine-based electron acceptor (**TRZ**) to form nanorods in water, leading to the observation of greenish CT emission with long lifetime ($\tau = 0.92 \mu\text{s}$). As for another electron donor (**QaAc**) with similar structure but enhanced water-solubility and poor aggregation ability, water-soluble pillar[5]arene (**WP5**) could be introduced to promote the aggregation process, thus resulting in the CT emission with long lifetime ($\tau = 0.61 \mu\text{s}$). The formation of nanoaggregates not only shortens the distance between the donor and acceptor to promote charge transfer process, but also reduces the adverse effects of external oxygen on the CT emission. In addition, structural modification of the acceptor with substituent groups bearing stronger electron-accepting abilities would cause obvious red-shift of the emission, which allows the convenient construction of long lifetime organic luminescent materials with different emission colors.

BrAc, a typical dimethylacridine-based electron donor, was first synthesized by using 9,10-dihydro-9,9-dimethylacridine and 4-bromobenzaldehyde as the starting materials (Scheme S1 and Figs. S1–S6 in Supporting information). The long alkyl chain of **BrAc** was designed to increase the stability of nanoaggregates in aqueous solution. It has been widely reported that CT materials showing long lifetime can be successfully constructed when dimethylacridine-based electron donors and triazine-based electron acceptors are covalently modified on the side chains of polymers [24–26]. Hence, a triazine-based derivative (**TRZ**) was selected as acceptor and it was inferred that the system would exhibit CT emission with long lifetime when **BrAc** and **TRZ** co-aggregated to form abundant nanoaggregates through π - π interaction and hydrophobic interaction in aqueous phase.

To verify the above assumption, the self-aggregate behavior of **BrAc-TRZ** complex in water was explored. **BrAc-TRZ** solution showed obvious Tyndall effect, suggesting the existence of abundant nanoaggregates. The morphology and size of the nanoaggregates formed by **BrAc-TRZ** complex were determined by transmission electron microscopy (TEM) and dynamic light scattering (DLS) measurements, respectively. The corresponding results revealed the formation of large-sized nanorods with an average diameter of

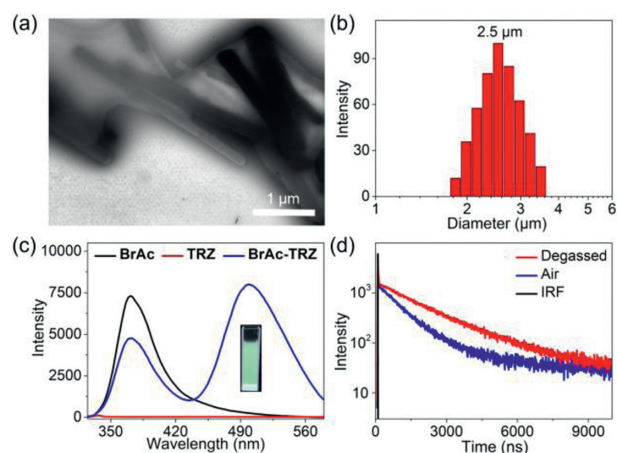


Fig. 1. TEM image (a) and DLS data (b) of **BrAc-TRZ** nanoaggregates. (c) PL spectra of **BrAc**, **TRZ**, and **BrAc-TRZ** in water ($\lambda_{\text{ex}} = 300 \text{ nm}$). Inset: PL images of **BrAc-TRZ** in water. (d) Transient PL decay spectra of **BrAc-TRZ** nanoaggregates at 499 nm in air and after degassed ($\lambda_{\text{ex}} = 300 \text{ nm}$). IRF: Instrument response function. [**BrAc**] = 250 $\mu\text{mol/L}$, and [**TRZ**] = 20 $\mu\text{mol/L}$.

2.5 μm (Figs. 1a and b). Subsequently, photoluminescence (PL) performance of **BrAc-TRZ** aggregates in water was studied. As shown in Fig. 1c, **TRZ** was basically not emissive, but the **BrAc-TRZ** co-aggregates showed strong greenish fluorescence with a maximum emission peak at 499 nm, which displayed red-shifted emission relative to **BrAc** ($\lambda_{\text{em,max}} = 371 \text{ nm}$). Upon gradually increasing the concentration of **TRZ**, the fluorescence intensity of **BrAc** at 371 nm decreased, while the emission peak at 499 nm increased (Fig. S12 in Supporting information). The above phenomena suggest distinct intermolecular charge transfer between **BrAc** and **TRZ** has taken place, which is similar to the phenomena in the reported literature [24]. Then, transient PL decay spectra in water were measured under different conditions. With respect to free **BrAc**, the average lifetime (τ) was below 5 ns (Fig. S13 in Supporting information). **TRZ** is not emissive, hence the spectrum was absent. However, for the **BrAc-TRZ** aggregates in air and after degassed, the average lifetime (τ) was 0.92 μs and 1.78 μs , respectively (Fig. 1d), which showed obvious long lifetime emission compared with free **BrAc**.

For in-depth understanding the PL properties of **BrAc-TRZ** aggregates, the absorption and excitation spectra were measured (Fig. S14 in Supporting information). The absorption spectrum of **BrAc-TRZ** aggregates was a simple overlay of **BrAc** and **TRZ**. No new absorption peak appeared, which confirmed that weak intermolecular interaction occurred between **BrAc** and **TRZ** in the ground state. In addition, the excitation spectrum of **BrAc-TRZ** aggregates matched well with that of free **BrAc**, which indicated the above two systems have the same excitation pathway [30]. Based on the above experiments, we inferred that the emission at 499 nm might be attributed to the charge transfer in the excited state [31,32]. Moreover, the photoluminescence quantum yield (PLQY) of **BrAc-TRZ** aggregates was measured to be 19.70% by integrating sphere (Fig. S18 in Supporting information).

To further understand the mechanism of CT emission, PL behavior of **BrAc-TRZ** in good solvent (THF) was further studied. Compared with free **BrAc** and **TRZ**, the appearance of new emission peak could not be observed in the PL spectra of **BrAc-TRZ**, implying that no charge transfer occurred (Fig. 2a). In addition, transient PL decay spectra revealed that the average lifetime (τ) of **BrAc-TRZ** in THF was below 5 ns no matter in air or after degassed, indicating no long lifetime emission in the above system (Fig. 2b). Therefore, it could be concluded that the CT emission of **BrAc-TRZ** with long lifetime in water was attributed to the formation of nanoaggregates, which can shorten the distance between the donor and

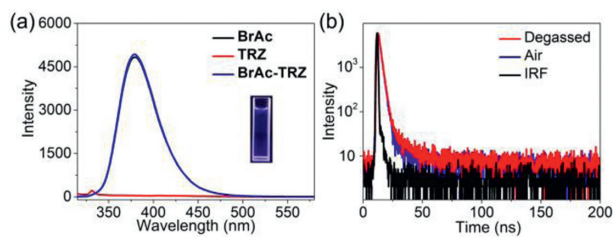


Fig. 2. (a) PL spectra of **BrAc**, **TRZ**, and **BrAc-TRZ** in THF ($\lambda_{\text{ex}} = 300$ nm). Inset: PL images of **BrAc-TRZ** in THF. (b) Transient PL decay spectra of **BrAc-TRZ** at 380 nm in air and after degassed in THF ($\lambda_{\text{ex}} = 300$ nm). IRF: Instrument response function. [**BrAc**] = 250 $\mu\text{mol/L}$, and [**TRZ**] = 20 $\mu\text{mol/L}$.

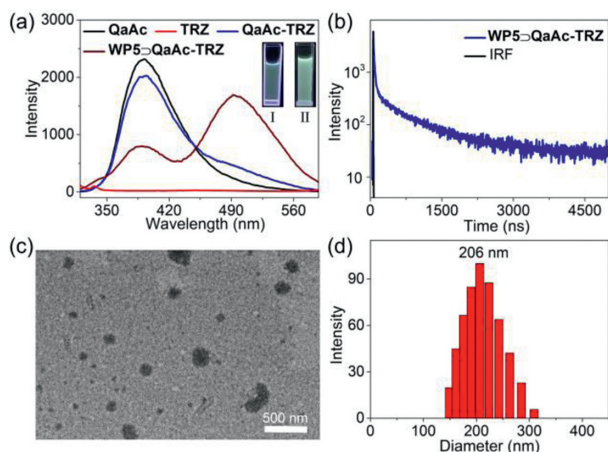


Fig. 3. (a) PL spectra of **QaAc**, **TRZ**, **QaAc-TRZ**, and **WP5-QaAc-TRZ** in water ($\lambda_{\text{ex}} = 300$ nm). Inset: PL images of **QaAc-TRZ** (I) and **WP5-QaAc-TRZ** (II) in water. (b) Transient PL decay spectra of **WP5-QaAc-TRZ** at 492 nm in water ($\lambda_{\text{ex}} = 300$ nm). IRF: Instrument response function. TEM image (c) and DLS data (d) of **WP5-QaAc-TRZ** nanoassemblies. [**WP5**] = 31.25 $\mu\text{mol/L}$, [**QaAc**] = 250 $\mu\text{mol/L}$, and [**TRZ**] = 20 $\mu\text{mol/L}$.

acceptor to induce efficient charge transfer. This is also consistent with our assumption. In addition, considering that CT materials showing long lifetimes are related to the long-lived triplet excited (T_1) state, which can be quenched by oxygen, it is also proposed that the aggregation process can reduce the adverse effect of oxygen on CT emission [14,24].

Considering that the excellent aggregation ability of **BrAc-TRZ** complex in water was the key point to induce CT emission, it was questioned whether the complex could still exhibit CT emission when the water-solubility of electron donor was increased. To answer this question, another electron donor (**QaAc**) with better water-solubility while poor aggregation ability was synthesized by quaternization reaction of **BrAc** (Scheme S1 and Figs. S7–S9 in Supporting information). Then, the aggregate behavior of **QaAc-TRZ** complex in water was explored. **QaAc-TRZ** complex showed weak opalescence in water and the optical transmittance at 600 nm was nearly to 98% (Fig. S16 in Supporting information), indicating its very limited aggregation behavior. PL spectra revealed that **QaAc-TRZ** showed no obvious new emission peak compared with free **QaAc** (Fig. 3a), implying the charge transfer efficiency was low, and the CT emission was quite weak under this condition.

It has been widely reported that water-soluble pillar[5]arene (**WP5**) can bind with the quaternary ammonium group of different guest molecules and induce the formation of various nanostructures [33–35]. Hence, it was inferred that a large number of nanoaggregates could form upon the strong host-guest interaction between **WP5** and **QaAc**, resulting in the strong CT emission with long lifetime. To verify this assumption, the binding behavior between **WP5** and **QaAc** was firstly investigated. Since the

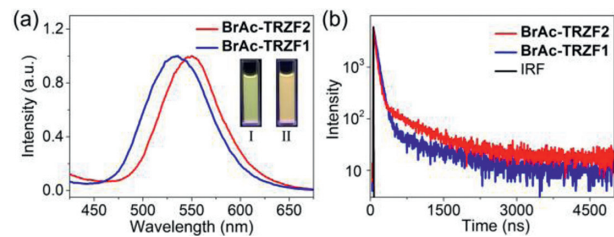


Fig. 4. (a) PL spectra of **BrAc-TRZF1**, **BrAc-TRZF2** in water ($\lambda_{\text{ex}} = 300$ nm). Inset: PL images of **BrAc-TRZF1** (I) and **BrAc-TRZF2** (II). (b) Transient PL decay spectra of **BrAc-TRZF1** at 536 nm and **BrAc-TRZF2** at 550 nm in water ($\lambda_{\text{ex}} = 300$ nm). IRF: Instrument response function. [**BrAc**] = 250 $\mu\text{mol/L}$, [**TRZF1**] = 20 $\mu\text{mol/L}$, and [**TRZF2**] = 20 $\mu\text{mol/L}$.

strong absorption of **QaAc** below 320 nm would disturb the UV-vis titration measurement, amyltrimethylammonium bromide (**G_M**) with the same binding site of **QaAc** was taken as a model guest molecule. Job's plot indicated that **WP5** and **G_M** could form host-guest complex with a 1:1 stoichiometry (Fig. S15 in Supporting information). The self-aggregate behavior of **WP5-QaAc-TRZ** assemblies was further explored. Compared with free **QaAc-TRZ** solution, **WP5-QaAc-TRZ** solution showed notable opalescence as well as obvious Tyndall effect. Moreover, the transmittance of **WP5-QaAc-TRZ** at 600 nm was much lower than that of **QaAc-TRZ** solution (Fig. S16 in Supporting information). The above phenomena were mainly attributed to the macrocyclic host **WP5**-promoted aggregation of guest molecule. DLS result and TEM image revealed that **WP5-QaAc-TRZ** complex could form nanoparticles with an average diameter of 206 nm (Figs. 3c and d). As presented in Fig. 3a, when **WP5** was added into the **QaAc-TRZ** solution, the fluorescence emission intensity at 394 nm decreased significantly, while the emission intensity at 492 nm increased obviously, suggesting the efficient charge transfer between **QaAc** and **TRZ** has taken place. As expected, transient PL decay spectra revealed that the **WP5-QaAc-TRZ** assemblies displayed a long lifetime emission ($\tau = 608.2$ ns) (Fig. 3b). The above phenomena further proved that the aggregation behavior is a critical factor for the fabrication of CT materials with long lifetime based on supramolecular strategy.

CT materials with long-wavelength emission could be conveniently constructed by modifying the acceptor with substituent groups possessing stronger electron-accepting abilities. **TRZF1** and **TRZF2** were designed as acceptors due to the high electron affinity of trifluoromethyl (Schemes S2 and S3, Figs. S10 and S11 in Supporting information). Free **TRZF1** and **TRZF2** were both basically not emissive in water (Fig. S17 in Supporting information). However, when the donor and acceptor co-aggregated into nanoaggregates, strong CT emission could be induced, and the emission colors could range from original green (499 nm) to orange (550 nm) (Fig. 4a). The CT emission of **BrAc-TRZF1** and **BrAc-TRZF2** also exhibited long lifetime, which was 264.2 ns and 413.6 ns, respectively (Fig. 4b). In addition, PLQY was measured to be 17.22% and 13.58%, respectively (Fig. S18 in Supporting information).

In summary, novel aggregation-induced charge transfer (CT) emission systems with long lifetime directed by supramolecular strategy have been successfully developed in aqueous phase. For the electron donor (**BrAc**) with excellent aggregation ability, it can co-aggregate with the electron acceptor (**TRZ**) to form nanorods in water, leading to the obvious CT emission with long lifetime ($\tau = 0.92$ μs). As for the electron donor (**QaAc**) with poor aggregation ability, **WP5** can be added to promote the aggregation process, resulting in the CT emission with long lifetime ($\tau = 0.61$ μs). The formation of nanoaggregates can not only promote the charge transfer between the electron donor and acceptor, but also can reduce the adverse effects of external oxygen on the CT emission. In addition, CT materials with different emission colors can be

conveniently constructed by replacing the acceptor with different electron-accepting capabilities. The present work provides a new strategy for the construction of long lifetime organic luminescent materials, which might have potential applications in the fields of time-resolved fluorescence imaging and photocatalysis.

Declaration of competing interest

The authors report no declarations of interest.

Acknowledgments

We thank Prof. Youxuan Zheng and Dr. Guangping Sun for assistance with data analyses. This work was supported by the National Natural Science Foundation of China (No. 21871136), the Natural Science Foundation of Jiangsu Province (No. BK20211179), and the Fundamental Research Funds for the Central Universities (No. NE2019002).

Supplementary materials

Supplementary material associated with this article can be found, in the online version, at doi:10.1016/j.ccllet.2021.09.070.

References

- [1] H. Zhu, H. Wang, B. Shi, et al., *Nat. Commun.* 10 (2019) 2412.
- [2] T. Xiao, J. Wang, Y. Shen, et al., *Chin. Chem. Lett.* 32 (2021) 1377–1380.
- [3] J. Chen, Y. Zhang, Z. Meng, et al., *Chem. Sci.* 11 (2020) 6275–6282.
- [4] N. Song, Z. Zhang, P. Liu, et al., *Adv. Mater.* 32 (2020) 2004208.
- [5] Y. Liu, Y. Liao, P. Li, Z.T. Li, D. Ma, *ACS Appl. Mater. Interfaces* 12 (2020) 7974–7983.
- [6] X.H. Wang, X.Y. Lou, T. Lu, et al., *ACS Appl. Mater. Interfaces* 13 (2021) 4593–4604.
- [7] G. Sun, W. Qian, J. Jiao, et al., *J. Mater. Chem. A* 8 (2020) 9590–9596.
- [8] A.J.P. Teunissen, C. Pérez-Medina, A. Meijerink, W.J.M. Mulder, *Chem. Soc. Rev.* 47 (2018) 7027–7044.
- [9] J.J. Li, H.Y. Zhang, X.Y. Dai, Z.X. Liu, Y. Liu, *Chem. Commun.* 56 (2020) 5949–5952.
- [10] M. Kownacki, S.M. Langenegger, S.X. Liu, R. Häner, *Angew. Chem. Int. Ed.* 131 (2019) 761–765.
- [11] X. Liu, K. Wang, M. Externbrink, et al., *Chin. Chem. Lett.* 31 (2020) 1239–1242.
- [12] P.P. Jia, L. Xu, Y.X. Hu, et al., *J. Am. Chem. Soc.* 143 (2021) 399–408.
- [13] W. Chen, F. Song, *Chin. Chem. Lett.* 30 (2019) 1717–1730.
- [14] Z. Zhu, D. Tian, P. Gao, et al., *J. Am. Chem. Soc.* 140 (2018) 17484–17491.
- [15] Q. Zhang, S. Xu, M. Li, et al., *Chem. Commun.* 55 (2019) 5639–5642.
- [16] F. Ni, N. Li, L. Zhan, C. Yang, *Adv. Optical Mater.* 8 (2020) 1902187.
- [17] L. Yu, Z. Wu, G. Xie, et al., *J. Mater. Chem. C* 8 (2020) 12445–12449.
- [18] Y.F. Wang, M. Li, W.L. Zhao, et al., *Chem. Commun.* 56 (2020) 9380–9383.
- [19] J.P. Phelan, S.B. Lang, J. Sim, et al., *J. Am. Chem. Soc.* 141 (2019) 3723–3732.
- [20] T. Huang, W. Jiang, L. Duan, *J. Mater. Chem. C* 6 (2018) 5577–5596.
- [21] H. Tanaka, K. Shizu, H. Miyazaki, C. Adachi, *Chem. Commun.* 48 (2012) 11392–11394.
- [22] W. Hu, L. Guo, L. Bai, et al., *Adv. Healthc. Mater.* 7 (2018) 1800299.
- [23] Q. Zhang, H. Kuwabara, W.J. Potscavage, et al., *J. Am. Chem. Soc.* 136 (2014) 18070–18081.
- [24] S. Shao, J. Hu, X. Wang, et al., *J. Am. Chem. Soc.* 139 (2017) 17739–17742.
- [25] C.M. Tonge, Z.M. Hudson, *J. Am. Chem. Soc.* 141 (2019) 13970–13976.
- [26] J. Hu, Q. Li, X. Wang, et al., *Angew. Chem. Int. Ed.* 58 (2019) 8405–8409.
- [27] A.M. Polgar, J. Poisson, N.R. Paisley, et al., *Macromolecules* 53 (2020) 2039–2050.
- [28] C. Wu, W. Liu, K. Li, et al., *Angew. Chem. Int. Ed.* 133 (2021) 4040–4044.
- [29] Y.K. Wang, C.C. Huang, H. Ye, et al., *Adv. Optical Mater.* 8 (2019) 1901150.
- [30] L. Liu, X. Wang, S. Zhu, et al., *Dyes Pigm.* 166 (2019) 416–421.
- [31] X. Wang, L. Liu, S. Zhu, J. Peng, L. Li, *RSC Adv.* 7 (2017) 40842–40848.
- [32] M. Sarma, K.T. Wong, *ACS Appl. Mater. Interfaces* 10 (2018) 19279–19304.
- [33] H. Zhang, Z. Liu, Y. Zhao, *Chem. Soc. Rev.* 47 (2018) 5491–5528.
- [34] P. Li, Y. Chen, Y. Liu, *Chin. Chem. Lett.* 30 (2019) 1190–1197.
- [35] W. Feng, M. Jin, K. Yang, Y. Pei, Z. Pei, *Chem. Commun.* 54 (2018) 13626–13640.